

# PIRE-GEMADARC Internal Notes – Germanium Internal Amplification (GeIA):

\*

Chih-Hsiang Yeh

*Institute of Physics, Academic Sinica, Nangang, Taipei, Taiwan and  
Department of Physics, National Central University, Chungli, Taoyuan, Taiwan<sup>†</sup>*

(PIRE-GEMADARC Collaboration)

(Dated: April 22, 2021)

To understand the solid-state physics related to the crystal for the germanium internal amplification at two conventional temperatures, liquid nitrogen temperature(77K) and liquid helium temperature(4K), some of the literature studies are completed with the content summarized in this note.

## CONTENTS

I. Introduction	1
II. A brief introduction of p-n junction	2
III. Signal Amplification	2
A. Necessary Electron-related Parameters:	2
1. Electrical Mobility( $\mu$ )	2
2. Effective mass( $m^*$ )	2
3. Relaxation Time( $\tau$ )	3
B. Ionization rate	3
C. Pioneer: Russian investigation[2000]	3
IV. Noise in the Crystal	4
A. Bulk leakage current	4
B. Contact leakage current	5
C. Surface leakage current	5
D. Summary for three currents	5
V. Performance for the Detector	6
A. Working model I for Gain	6
B. Working model II for Gain	7
C. Electrical Breakdown	8
VI. Conclusion	9
VII. Unsolved issues	9
VIII. Acknowledgement	10
References	10

## I. INTRODUCTION

Since some of the experiments, such as the low-mass WIMP search with  $\chi N$  scattering, require the low-threshold detector for detecting the small amount of energy, the fundamental laws of internal amplification,

which can be utilized for enlarging the signal, should be understood for getting the detector to be manageable.

In 2000, two experts from Russia, who are the pioneers of our research, came up with the conceptual design about applying the high voltage on the Ge detector and producing the electron-hole pairs that can be enhanced within the avalanche region in the crystal. Ever since, a bunch of experiments attempted to extend the idea and to see whether the idea can work out with the state-of-the-art technology in reality were carried out.

In our collaborations, two teams are realizing the notion under two conventional temperatures, which are 4K(University of South Dakota) and 77K(Tsing Hua University). Under these two different temperatures, the phenomenon happening to signal and noise in the crystal would be disparate. The studies are expected to figure out the difference between these two setups, and the advantage versus disadvantage in a variety of facets to them.

In the following sections, first, some of the basic knowledge related to the p-n junction would be introduced as the foundation of this research. Then, the internal amplification on the signal under these two temperatures mentioned will be elaborated. As the signal is strengthened, in parallel, the noise of the crystal could be unexpectedly magnified consequently. Since the signal-to-noise ratio is the ultimate criteria to compare between different setups, how to deal with the high noise originating from three species of leakage currents in the crystal is the very next topic that should be addressed.

At the end of the notes, first the calculation of the gain factor, which is based on the authentic electric field distribution in the P-type point contact(PPC) detector, would be regarded. Hereafter, in order to deal with the thorny problem on the dielectric breakdown, which is due to the tremendously high electric field and can sabotage the crystal intrinsically for both temperatures, the mechanism of the dielectric breakdown would be delivered to assess the crucial maximum voltage.

\*

<sup>†</sup> a9510130375@gmail.com

## II. A BRIEF INTRODUCTION OF P-N JUNCTION

The semiconductors may contain different impurity and usually there are two different groups of semiconductors: the n-type(electron-dominated) and the p-type(hole-dominated). For any crystal containing both types of semiconductors, the properties of the p-n junction can occur.

In Fig.1, a typical p-n junction is illustrated. On the p-n junction, the dynamic of the electron-hole diffusion and attraction, will start emerging in the crystal. After the electrons and the holes reach an equilibrium, the neutral region called "the depletion region" with the a stable electric field and without free charge carriers will show up. In the reverse-bias case, the higher the voltage, the larger the region it will be. In the end, the voltage should be enhanced to the one which can deplete the whole crystal, implying the whole crystal is turned into the neutral one. Afterward, this "neutral" crystal can be used to detect particles.

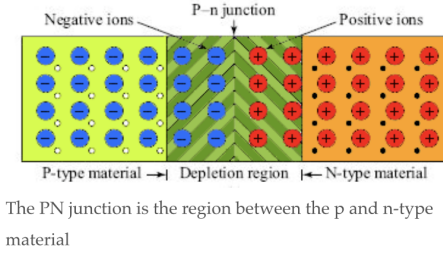


FIG. 1. The basic P-N Junction.

Then, the voltage applied to fully deplete the crystal can be derived from the formula as follows:

$$x_d = \sqrt{\frac{2\epsilon V_d}{qN_a}} \quad (1)$$

where  $x_d$  is the depletion length,  $N_a$  is the impurity concentration,  $V_d$  is the voltage solicited to do the task of the depletion. After moving some of the parameters from right to left, then the depletion voltage can be demonstrated clearly:

$$V_d = \frac{x_d^2 q N_a}{2\epsilon} \quad (2)$$

In FIG.2, the depletion voltage under the various temperatures for a detector with a length of 2.37cm is displayed. When the temperature becomes lower, the depletion voltage will be decreased.

If the detail of the fundamental physics in semiconductor is desired, chapter7 and chapter8 of the book[1] are recommended.

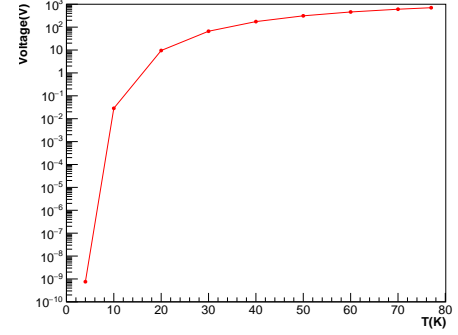


FIG. 2. The depletion voltage as a function of the temperature for the detector with the length equal to 2.37cm.

## III. SIGNAL AMPLIFICATION

### A. Necessary Electron-related Parameters:

At the start, let us visualize "an electron", which is ionized by a WIMP, flowing in the crystal. Many necessary parameters must be acquired in advance from this electron to unfold our studies. All of them will be depicted in the following subsections.

#### 1. Electrical Mobility( $\mu$ )

The definition of electrical mobility is as follows:

$$\mu = \frac{V_d(1 + \frac{E}{E_{sat}})}{E} \quad (3)$$

where  $V_d$  is the velocity of the electron,  $E$  is the electric field applied to the crystal, and  $E_{sat}$  is the saturation electric field which can make the velocity of the electron achieve the saturation one.

The mobility is estimated by the formula above. Specially, since in our experiment, the ultra-high electric field is applied, the saturation phenomenon, referring to the situation that the velocity would be a constant when the electric field is beyond the critical one, can be obtained. Fig.3[2] shows that when the electric field is above 10<sup>4</sup>V/cm, which is also the critical electric field in calculating the ionization rate described in the latter section, the velocity of the electron is a constant for both temperatures.

#### 2. Effective mass( $m^*$ )

Under the different temperatures, the effective conductivity masses are varying. Fig.4[3] displays that the hole has the higher effective mass when the temperature is low. Since there is no such study for Ge, the study of silicon is taken as an instance to picture the tendency for

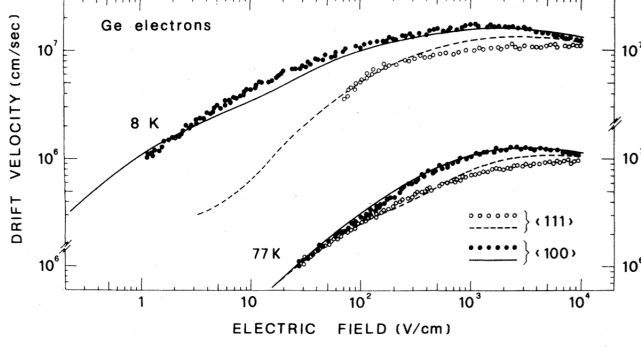


FIG. 3. The drift velocity as a function of electric field is shown for two temperatures.

the effective masses of the electron and the hole. In our studies, the effective mass of the electron is simply set to be  $m = 0.12m_0$  and for the hole, the effective mass is simply set to be  $m = 0.21m_0$ ,  $m_0$  is the mass of the electron.

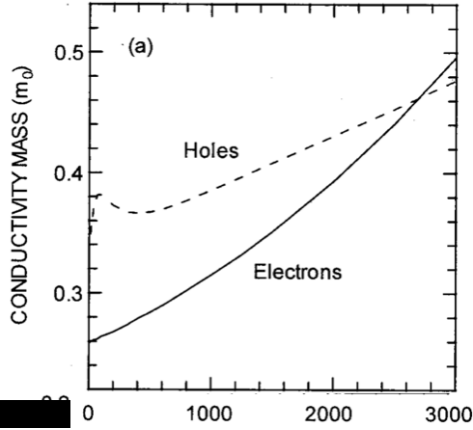


FIG. 4. The relation between the effective mass( $m_0$ ) and the temperature( $T$ ) is demonstrated for both electron/hole in Si.

### 3. Relaxation Time( $\tau$ )

The period of time that the electron can survive without bumping into another atom:

$$\tau = \frac{\mu \times m^*}{e} \quad (4)$$

$e$  is the elementary charge,  $\mu$  is the mobility of the electron, and  $m^*$  is the effective mass.

After acquainting the relaxation time, the next thing that should be figured out is the mean free path( $L$ ), which means how far the electron can go without

running into another atom in the crystal. The formula is as follows:

$$L = \tau \times V_d \quad (5)$$

$V_d$  means the velocity of the electron, and  $\tau$  is the relaxation time.

The parameters which are discussed in this section would be utilized in the next section for developing the theory of amplifying the signal.

### B. Ionization rate

The ionization rate is defined as the following description: How many electrons/holes can be ionized within 1cm?

After depleting the crystal, next the relation between the ionization rate and the  $E(\text{V/cm})$  can be brought to light. Based on the formulae (6),(7) and (8) from paper[4], the ionization rate can be decided by exploiting the mean free path( $L$ ), electric field( $E(x)$ ) and ionization energy( $U$ ) of the material,

$$\alpha_s = \frac{a_s}{z} \exp\left\{-\frac{b_s}{E(x)}\right\} \quad (6)$$

$$z(x) = 1 + \frac{b_n}{E(x)} \exp\left\{-\frac{b_n}{E(x)}\right\} + \frac{b_p}{E(x)} \exp\left\{-\frac{b_p}{E(x)}\right\} \quad (7)$$

$$a_s = \frac{1}{L_s}, b_s = \frac{U_s}{qL_s}, s = \{p, n\} \text{ type} \quad (8)$$

$\alpha_s$  means the ionization rate,  $E(x)$  is the electric field distribution in the crystal,  $L_s$  is the mean free path[5], and  $U_s$  means the ionization energy, which is set 3eV as measured in this paper[6].

FIG.5 can be framed by employing the formulae introduced above. It gives us the evidence that  $10^4 \text{ V/cm}$  is the critical electric field as the ionization rate significantly increases when the electric field is above that value. Besides, because the curves for holes are higher than the curves for electrons at both temperatures, by and large, the hole can give us more signal.

### C. Pioneer: Russian investigation[2000]

In light of the paper[7], the conceptual design on the coaxial detector with High Purity Germanium(HPGe), which is displayed in FIG.6, is provided. In order to estimate the gain factor, which is a criteria for

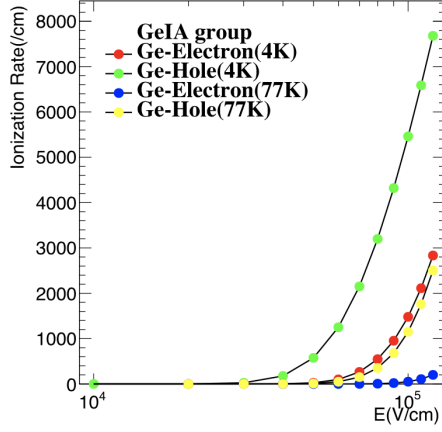


FIG. 5. The ionization rates for both electron and hole under both 4K and 77K.

the performance of the detector as described in the end of this note, the electric field distribution in the detector should be recognized beforehand. The distributions in the strip detector can be illustrated with the impurity concentration as the following formula:

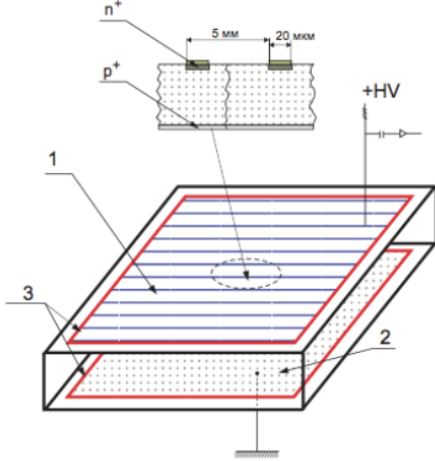


FIG. 6. Germanium detector with an internal amplification (schematic view): (1) anode strips, (2) cathode, and (3) guard electrodes. The scheme of n+ and p+ layers is shown in the upper part of the figure.

$$E(r) = \frac{Ne}{2\epsilon}r - \frac{V + \frac{Ne}{4\epsilon}(R_2^2 - R_1^2)}{r \ln(\frac{R_2}{R_1})} \quad (9)$$

where  $N$  is the impurity concentration,  $e$  is the electron charge,  $\epsilon$  is the dielectric constant of the germanium,  $R_2$  and  $R_1$  are the radii of the cathode and the anode, and  $V$  is the applied voltage.

Based on the calculation by Formula9, Fig.7 demonstrates the electric fields for different impurity concen-

trations. According to FIG.5, when the electric field is higher than  $10^4$ (V/cm), the number of electrons will be increased as a function of the electric field. As a result of that, two regions can be separated with this critical electric field.

1. Avalanche region: When the electric field is above  $10^4$ (V/cm), the avalanche effect will emerge, subsequently, the signal will be amplified.
2. Reach-through region: If the electric field is below the critical one, the electron/hole will just go through normally without any effect.

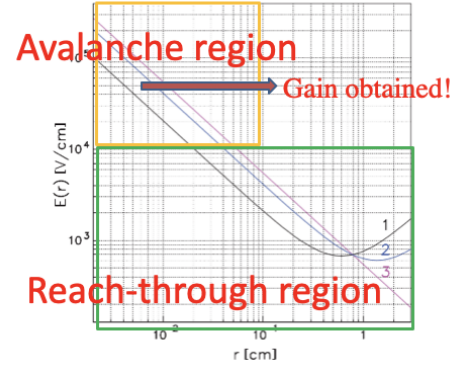


FIG. 7. The electric field as a function of the distance from the strip in FIG.6 with the different impurities. The numbers above the lines mean the different impurities: (1) $10^{10}cm^{-3}$ , (2) $4 \times 10^9 cm^{-3}$  and (3)  $0 cm^{-3}$

These studies give out a clue that the detector can be devised to yield the amplification of the signal with the electric field above a certain level.

#### IV. NOISE IN THE CRYSTAL

Unfortunately, the noise in the crystal is inevitable. The genres of the noise in the crystal should be characterized as the criteria for the limitation on measuring the lowest dark matter mass theoretically. There are three sorts of noise in the crystal: the bulk leakage current, the contact leakage current, and the surface leakage current. In the following paragraph, all of them are described individually.

##### A. Bulk leakage current

Due to the thermal fluctuation, the electrons from the bulk(purity, such as Ge) material may be ionized. Fortunately, the level of this noise can be ignored below

77K. The associated information is well-written in the formula(13)[8]:

$$I = A e^{\frac{-E_{\text{Ge Band}}}{2k_B T}} * q * \frac{1}{t} \quad (10)$$

A is the intrinsic concentration,  $E_{\text{Ge Band}}$  is the band gap of Ge, q is the coulomb constant, T is the temperature(K), and t is the period of the time the electron/hole would come to the detector.

### B. Contact leakage current

Because of the barrier between the semiconductor and the metal as well as thermal fluctuation, there is a possibility that the electron in the conductive band could leap into the metal, leading to unwanted dark current.

Fig.8[9], which is the measurement from USD, gives out the scale of the contact leakage current at 100K is around  $5 \times 10^{-10}$  A. Compared with the Fig.9[10], which is demonstrated by other group with the a-Ge detector, the results at 100 K are similar. Upon the usage of FIG.9, the contact leakage current under 77K, which is around  $5 \times 10^{-16}$  A/cm<sup>2</sup>. can be extrapolated.

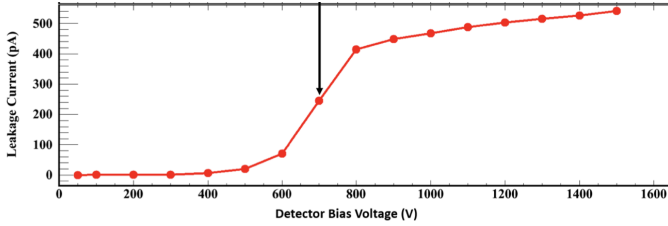


FIG. 8. The determination of full depletion voltage for detector USD-L01 using I-V measurements at 100 K.

The fundamental physics is "Schottky effect", which is a kind of the thermal emission. The simplified formula can be expressed with the "Richardson's law" as follows:

$$I \propto T^2 e^{\frac{W}{k_B T}} \quad (11)$$

T is the temperature(K), W is the work function of the material, and  $k_B$  is the Boltzmann constant.

The detail of this mechanism is compiled in the book[11]. Basically, it is a Metal-Semiconductor junction problem, which is a very big topic authentically and the chapter 10, 11 of book[11](Strongly recommended!) and chapter 6 and 7 of book[12] are recommended to acquire more detail on the related topic.

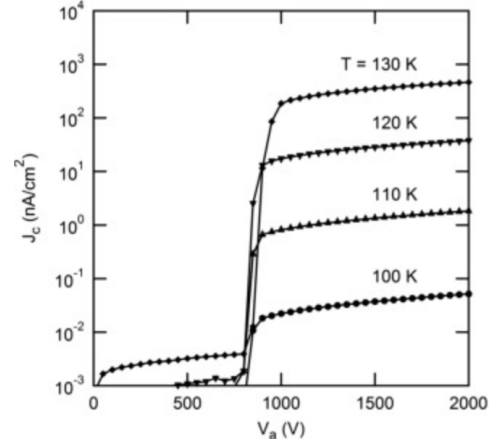


FIG. 9. Measured center contact leakage current density plotted as a function of bias voltage at various temperatures for an a-Ge/HPGe/a-Ge detector

### C. Surface leakage current

It depends on the quality of the crystal. By and large, lowering the temperature can help get rid of the noise.

There are two papers depicting the measurement on the surface leakage current for Ge. Please look at Fig.10[13], which shows the surface leakage current from InAs Avalanche Photodiodes. Although this is not for Ge, it gives us a hint on the scale of the semiconductors. The points(■) can be expanded in the figure to predict the surface leakage current under more lower temperatures. The extremely low surface leakage current can be inferred in this paradigm under the low temperature.

Currently, the new results on the surface leakage current of a-Ge from USD are published. Amazingly, In FIG.11[14], the leakage current is projected down to the temperature at 4K, and the considerably low leakage current is illustrated at the very low temperature, leading to the feasibility for detecting the low-mass dark matter.

### D. Summary for three currents

In FIG.12, the chart for summarizing these three currents under the saturation circumstance are displayed. Overall, the surface leakage current is the severe conundrum for any temperature. At 77K, the contact leakage current is competitive with the surface leakage

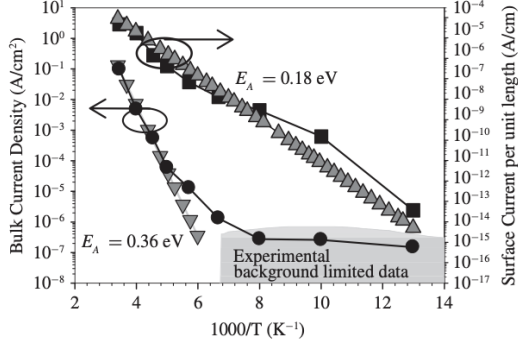


FIG. 10. The surface leakage current, which is remarked by (■), is measured with the InAs Avalanche Photodiodes.

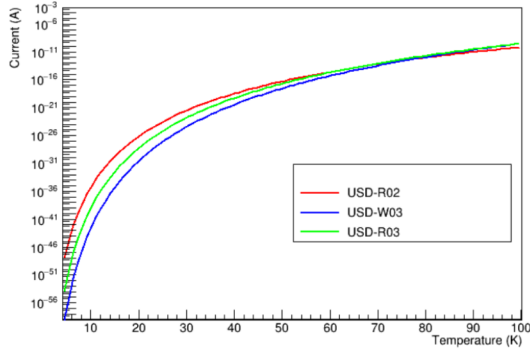


FIG. 11. Projected variation of the surface leakage current with temperature for a PPC detector using the parameters obtained from the a-Ge used in detectors USD-R03, USD-R02 and USD-WO3. .

current, as their numbers are very close to each other. At 4K, surprisingly, the surface leakage current surpasses all others overwhelmingly.

## V. PERFORMANCE FOR THE DETECTOR

In this section, the performance of the detector is expected to be projected under both temperatures with the information at hand.

### A. Working model I for Gain

The gain factor can be estimated with two parameters, including the electric field and the ionization rate. Given the geometry of the detector, the gain factor can be obtained:

$$G = \int \alpha_s(E) \times E(r) dr \quad (12)$$

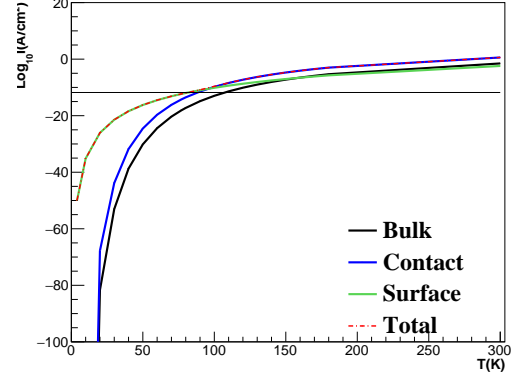


FIG. 12. The leakage current as a function of the temperature for three types of leakage currents.

In order to estimate the gain factor for the detector at both temperatures, the electric field distribution, which is geometry-dependent, should be identified in the different shapes of the detectors.

Since the electric field distributions at two temperatures are nearly the same under the same voltage in the strip detector, see Formula(9), the same pattern is assumed to be the tenet for the P-type point contact(PPC) detector, meaning that in our case, the electric field distribution is voltage-dependent and temperature-independent.

The electric field distribution in FIG13, which is given by the Akash's report(2018-08-09), is utilized in these studies. Since there is no direct result for the electric field under a bunch of the voltages in the PPC detector, the extrapolation with the strip detector is implemented. The relation in the following formula can be employed to predict the electric field under the different voltage in the PPC detector:

$$\text{Strip detector } \frac{E_{3500V}}{E_{xV}} = \text{PPC detector } \frac{E_{3500V}}{E_{xV}} \quad (13)$$

x is the desired voltage.

After fully plotting out the electric field distribution in the PPC detector, incorporating with the ionization rate portrayed in FIG.5, the predictions of gains under both temperatures can be demonstrated in FIG.14. The small conclusion framed by this plot is that the lower the temperature we use, the lower the voltage should be applied to the crystal for achieving the same gain below 1000. Furthermore, after zooming in the region from G=1 to G=3, which is exhibited in FIG.15, the clear point at 3500V for initiating the generation of the internal amplification can be observed under 77K. At 4K,1500V is claimed to kick off the process of the

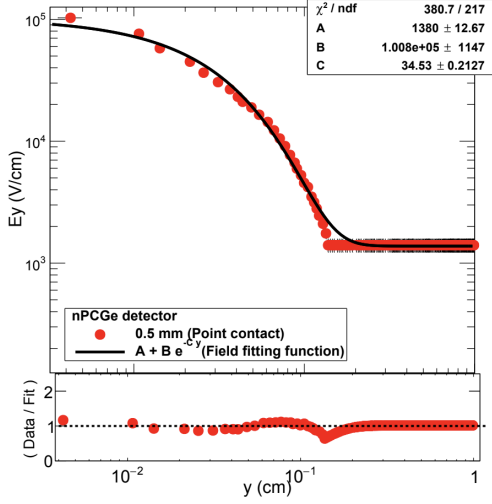


FIG. 13. The electric field distribution as a function of the radius.

internal amplification.

Albeit a lower voltage is required to attain the same gain at the lower temperature, the breakdown phenomenon, i.e. when the applied voltage exceeds the "break-down" voltage, should be well recognized for preventing our detector from being exterminated.

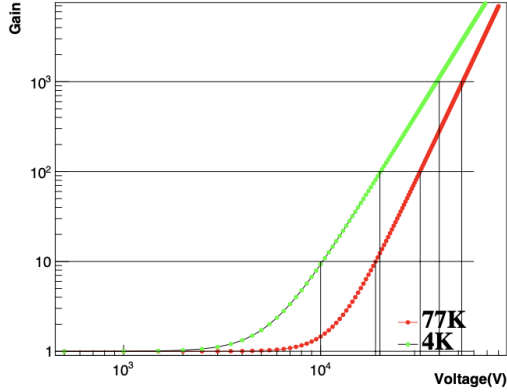


FIG. 14. The gain factor as a function of the voltage under these two temperatures.

### B. Working model II for Gain

After applying the ionization rates for the hole and the electron with the electric field to directly calculate the gain factor, the working model II, which is also based on the ionization rate, is adopted to see whether the results are the same as previous ones.

After a bunch of the theoretical calculation written in [15], the Miller's approximation for the gain factor can

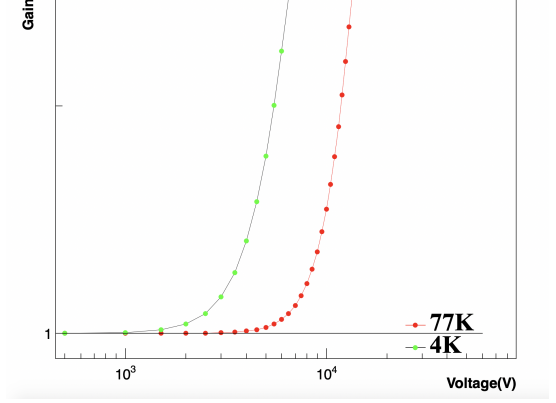


FIG. 15. The gain factor as a function of the voltage under these two temperatures.

be applied to our case:

$$M = \frac{1}{1 - \left(\frac{V}{V_{bk}}\right)^n} \quad (14)$$

where  $M$  is the multiplication factor,  $V$  is the applied voltage, and  $V_{bk}$  is the avalanche breakdown voltage.  $n$  is a constant depending on the material, doping, and primary carrier.

The results from the paper[16] show that when the resistivity is getting higher,  $n$  will become lower. In parallel, it has been suggested by other paper[17] that normally, the value of  $n$  for Ge is from 2 to 6. Since the current in our detector is assumed to be very low, resulting in the extremely high resistivity,  $n$  is simply set to be the lowest value within the normal region, which is 2.

The measurement done by the team of Prof. Dongming confirmed the value of  $V_{bk}$  to be 3000V at 4K for a PPC detector ( $r = 1\text{mm}$ ). Since a PPC detector ( $r = 0.5\text{mm}$ ) is expected to be utilized in our future experiment, the projection should be made to predict the breakdown voltage.

Figure16 shows the max electric field as a function of the voltage with the different radii of the contact points. First, since the breakdown voltage of a PPC detector ( $r = 1\text{mm}$ ) is measured already, the electric field causing the breakdown can be figured out. Then, under the same electric field, the voltage that would break down a PPC detector of which the radius of contact point is 0.5 mm can be obtained. This figure shows that a PPC detector ( $r = 0.5\text{mm}$ ) can break down at 700V.

In the end, as the breakdown voltage of a PPC detector ( $r = 0.5\text{mm}$ ) is established, the formula14 can be applied to do the same prediction as shown in Fig.14. Figure.17 displays the gain factor as a function of the



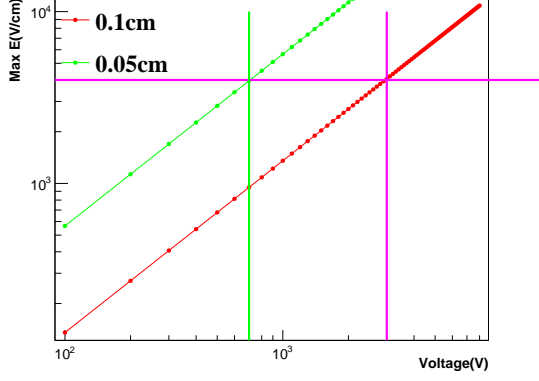


FIG. 16. The max electric field strength as a function of the voltage with the different radii of the contact points.

voltage with this formula. It shows that when the voltage is getting close to 700V, the gain factor will increase dramatically, leading to the problem of the stability.

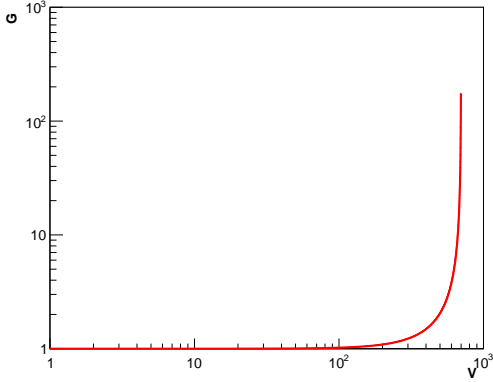


FIG. 17. The max electric field strength as a function of the voltage with the different radii of the contact points.

### C. Electrical Breakdown

The electrical breakdown can not only alter the electrical properties of the Ge atoms permanently, but also gives rise to the grave damage to the crystal. Therefore, the theoretical forecast on the breakdown voltage should be explored ahead of time for preserving our detector from being broken.

$E_{ds}$  obeys the following formula[18]:

$$E_{ds}(n, T) = C \times \sqrt[3]{\frac{nT}{2n}} \quad (15)$$

C is a constant determined by the experiment, T is the temperature, and n is the gain factor. If  $n > 1$ , it

means that the electrical breakdown is opened up under the high electric field.

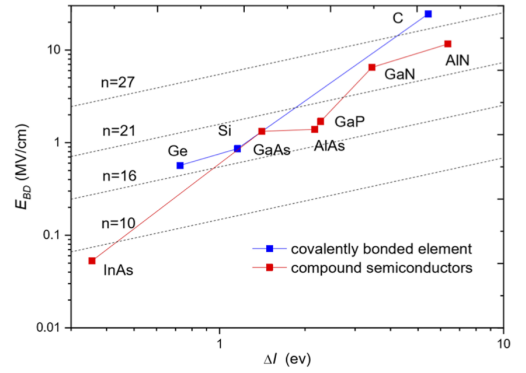


FIG. 18.  $\Delta I$  is the bandgap of the material, n is the gain factor,  $E_{BD}$  is the electrical strength.

In FIG.18[18], it shows that the breakdown electric field of Ge at 300K is around 0.5(MV/cm) when n equals 16. With respect to the difference for  $E_{ds}$  under two different temperatures, the calculation can be made as follows:

$$E_{ds}(T) = 0.6 \times \sqrt[3]{\frac{1 \times T \times 2^{16}}{16 \times 300 \times 2^1}} (MV/cm) \quad (16)$$

Since the same gain(Gain $\leq$ 1000) can be accomplished with the lower voltage at 4K as shown in FIG.14, along with the lower breakdown voltage as depicted above, the  $\frac{V}{V_{BD}}$  is introduced to compare how easily the breakdown could happen to the crystal at two temperatures relatively, where V corresponds to the voltage applied for a certain gain factor.

Since the highest electric field streaming in the detector can dictate the occurrence of the electrical breakdown, the highest electric field under the different voltage should be fully understood. In FIG.19, the electric field at  $r=0.05\text{mm}$ , the place on the surface of the contact, is shown as the supreme electric field in the detector. After using the formula(16) to calculate the breakdown  $E_{ds}$  under two temperatures, the matching voltage giving rise to the breakdown electric field can be grabbed by FIG.19.

In the end, as the voltages resulting in the different gains have already been sought in FIG.14, as well as the research on the voltages for the electrical breakdown under two temperatures are completed, next the comparison of  $\frac{V}{V_{BD}}$  can be offered. In TABLE.I, it shows the special pattern: at any gain, all of the ratios at 4K are higher than 77K, meaning that the detector can break down more easily at 4K.



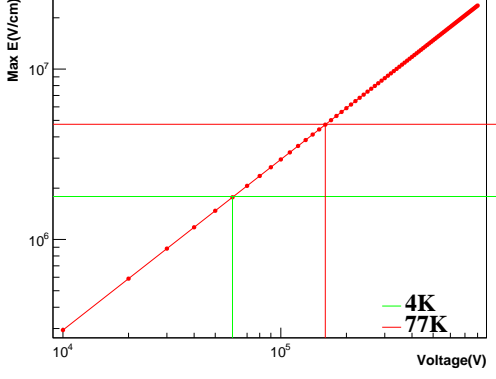


FIG. 19. The max electric field strength as a function of the voltage.

	G=10	G=100	G=1000
4K	0.16667	0.333	0.6667
77K	0.095	0.16	0.26

TABLE I.  $\frac{V}{V_{BD}}$  for a variety of gains under two temperatures.

## VI. CONCLUSION

In conclusion, evidently, if the temperature is reduced to 4K, the leakage currents will be subsided to the level that those contributions to the noise can be entirely ignored. But some strengths aren't always advantages, even though the same gain can be achieved with the lower voltage at 4K, the crystal should suffer from the risk of the lower breakdown voltage. At the moment, the experiment under 4K at USD is anticipated to produce the first stable version of germanium internal amplification.

## VII. UNSOLVED ISSUES

Actually, after our literature studies, some of the parameters are found contradictory between different papers. Some of the puzzles would be listed as follows:

1. Mean Free Path: In Akash's reports as well as the pioneer paper[7], the mean free path is set to be a constant for a given temperature without considering the effect of the electric field, but FIG.20, which is published by Prof. Dongming recently[19], shows that the mean free path can be changed by the electric field dramatically. In this document, the empirical formula for the mobility of the electron/hole is adopted to do the estimation, resulting in the changeable mean free path. But it is left for the audience.
2. Ionization Rate: Depending on the mean free path, the ionization rate also remains to be decided. In

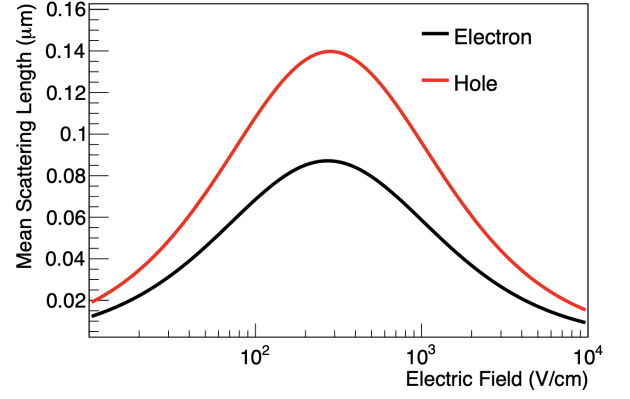


FIG. 20. Mean free scattering lengths for electrons and holes as a function of the electric field.

reality, the measurement should be done directly to determine the real value for the ionization rate. It is oversimplified to use the numbers given by other papers and put them in formulae (6) to (8) for getting the ionization rates.

3. Leakage Current: Since the measurements of leakage current are mostly done below 2000V, which is already above the depletion voltage, it is impossible to know the real numbers for all sorts of leakage currents when the applied voltage is above 3000V, which is required for making the gain factor bigger than 1. Although three constants can be assumed for three currents when the voltage is above the depletion one, the exact numbers for those are left to be measured.
4. Electrical Breakdown: The formulae written in this document for electrical breakdown are supposed to be right. Nevertheless, somehow the results in the paper describing these formulae can't be reproduced successfully. Unfortunately, I can't find another paper related to this issue. Conceivably, if the crystal is yielded to conduct the one-time research, no one will be willing to do this... This is also a part left to be concluded.
5. Contradiction between Model I and II: Two results given by the working model I and II are very disparate. Since there are too many parameters that should be used as the input of the working model I, the results could be extremely ridiculous if some of the parameters are not valid for a given temperature and a given electric field.

## VIII. ACKNOWLEDGEMENT

Thanks to Prof. Henry Wong at IoPAS on guiding me through the whole studies and providing me a lot of extraordinary advice on the direction of many issues. And

thanks to Prof. Dongming for answering me most of the problems originating from the published paper and as-

sisting me see whether the physical concepts I summarize are right.

- 
- [1] D. Neamen, *Semiconductor Physics And Devices*, 3rd ed. (McGraw-Hill, Inc., USA, 2002).
  - [2] C. Jacoboni, F. Nava, C. Canali, and G. Ottaviani, *Phys. Rev. B* **24**, 1014 (1981).
  - [3] D. M. Riffe, *J. Opt. Soc. Am. B* **19**, 1092 (2002).
  - [4] T. Lackner, *Solid-State Electronics* **34**, 33 (1991).
  - [5] Since the value of the mean free path is set a constant for a given temperature in the pioneer paper, we use 490nm for 77K and.
  - [6] W. Z. Wei, L. Wang, and D. M. Mei, *JINST* **12** (04), P04022, arXiv:1602.08005 [physics.ins-det].
  - [7] A. S. Starostin and A. G. Beda, *Physics of Atomic Nuclei* **63**, 1297 (2000).
  - [8] H. Chen, P. Verheyen, P. De Heyn, G. Lepage, J. De Coster, S. Balakrishnan, P. Absil, G. Roelkens, and J. Van Campenhout, *Journal of Applied Physics* **119**, 213105 (2016), <https://doi.org/10.1063/1.4953147>.
  - [9] W.-Z. Wei, X.-H. Meng, Y.-Y. Li, J. Liu, G.-J. Wang, H. Mei, G. Yang, D.-M. Mei, and C. Zhang, *Journal of Instrumentation* **13** (12), P12026.
  - [10] Q. Looker, M. Amman, and K. Vetter, *Nuclear Instruments and Methods in Physics Research Section A: Accelerators, Spectrometers, Detectors and Associated Equipment* **777**, 138 (2015).
  - [11] S. Li, *Semiconductor Physical Electronics* (Springer-Verlag, Berlin, Heidelberg, 2006).
  - [12] A. Milnes and D. Feucht, in *Heterojunctions and Metal Semiconductor Junctions*, edited by A. Milnes and D. Feucht (Academic Press, 1972) pp. 171 – 200.
  - [13] P. J. Ker, A. R. J. Marshall, A. B. Krysa, J. P. R. David, and C. H. Tan, *IEEE Journal of Quantum Electronics* **47**, 1123 (2011).
  - [14] S. Bhattarai, R. Panth, W. Z. Wei, H. Mei, D. M. Mei, M. S. Raut, P. Acharya, and G. J. Wang, *Eur. Phys. J. C* **80**, 950 (2020), arXiv:2002.07707 [physics.ins-det].
  - [15] C. D. Bulucea and D. C. Prisecaru, *IEEE Transactions on Electron Devices* **20**, 692 (1973).
  - [16] S. L. Miller, *Phys. Rev.* **99**, 1234 (1955).
  - [17] P. Spirito, *IEEE Transactions on Electron Devices* **21**, 226 (1974).
  - [18] L. Zhao, *AIP Advances* **10**, 025003 (2020).
  - [19] D. M. Mei *et al.*, *J. Phys. G* **47**, 105106 (2020), arXiv:1909.05806 [physics.ins-det].